THE JOURNAL OF BIOLOGICAL CHEMISTRY VOL. 281, NO. 51, pp. 39081–39087, December 22, 2006

Cyclophilin A Protects *Peg3* from Hypermethylation and Inactive Histone Modification*

Received for publication, July 14, 2006, and in revised form, September 29, 2006 Published, JBC Papers in Press, October 26, 2006, DOI 10.1074/jbc.M606687200

Ying-Chun Lu[‡], Jun Song[‡§], Hee-Yeon Cho[‡], Guoping Fan[¶], Kazunari K. Yokoyama[‖], and Robert Chiu[‡§1]**

*From the [‡]Dental Research Institute, UCLA School of Dentistry and [¶]Department of Human Genetics, UCLA, Los Angeles, California 90095, [‖]Gene Engineering Division, BioResource Center, RIKEN, Tsukuba, Ibaraki 305, Japan, **Department of Surgery/Oncology, UCLA School of Medicine, and [§]Jonsson Comprehensive Cancer Center, UCLA, Los Angeles, California 90095*

Imprinted genes are expressed from only one of the parental alleles and are marked epigenetically by DNA methylation and histone modifications. Disruption of normal imprinting leads to abnormal embryogenesis, certain inherited diseases, and is associated with various cancers. In the context of screening for the gene(s) responsible for the alteration of phenotype in *cyclophilin A* knockdown (*CypA*-KD) P19 cells, we observed a silent paternally expressed gene, *Peg3*. Treatment of *CypA*-KD P19 cells with the DNA demethylating agent 5-aza-dC reversed the silencing of *Peg3* biallelically. Genomic bisulfite sequencing and methylation-specific PCR revealed DNA hypermethylation in *CypA*-KD P19 cells, as the normally unmethylated paternal allele acquired methylation that resulted in biallelic methylation of *Peg3*. Chromatin immunoprecipitation assays indicated a loss of acetylation and a gain of lysine 9 trimethylation in histone 3, as well as enhanced DNA methyltransferase 1 and MBD2 binding on the cytosine-guanine dinucleotide (CpG) islands of *Peg3*. Our results indicate that DNA hypermethylation on the paternal allele and allele-specific acquisition of histone methylation leads to silencing of *Peg3* in *CypA*-KD P19 cells. This study is the first demonstration of the epigenetic function of CypA in protecting the paternal allele of *Peg3* from DNA methylation and inactive histone modifications.

DNA methylation regulates a number of biological processes, including genomic imprinting, X chromosome inactivation, silencing of tumor suppressor genes, and repression of retroviral elements (1, 2). Genomic imprinting relies on establishing and maintaining the parent-specific methylation of DNA elements that control the differential expression of maternal and paternal alleles (3, 4). Although the essential DNA methyltransferases and methyl-CpG-binding proteins have been discovered (5), proteins that regulate the establishment and maintenance of allele-specific methylation of DNA have not been identified. Nevertheless, data for an active role of DNA methylation in gene silencing are both correlative and functional. In addition, DNA methylation may occur in conjunction with histone modification to play a critical role in biallelic silencing through chromatin remodeling (6).

A number of human-inherited diseases linked to faulty methylation pathways and exhibiting abnormal development include Rett, immunodeficiency, centromeric heterochromatin instability, and facial anomalies, and X-linked α thalassemia/mental retardation syndromes (7–9). Moreover, aberrant methylation patterns are thought to be involved in tumorigenesis (10–13), causing genomic instability, abnormal imprinting, and deregulated expression of oncogenes or tumor suppressor genes.

The *Peg3* gene is one of several genes identified in an imprinted region mapped to human chromosome 19q13.4 (14). The mouse homolog of *Peg3* was the first imprinted gene identified from the proximal region of mouse chromosome 7 (15). Its high conservation between mice and humans suggests that it possesses critical cellular functions. *Peg3* appears to be ubiquitous, but the highest mRNA levels are found in placenta, uterus, ovary, brain, and testis (16). In mice, targeted disruption of the paternally inherited copy of *Peg3* eliminates *Peg3* expression. *Peg3*-negative heterozygous mice suffer growth impairment. Females display compromised nurturing behavior, resulting in a high death rate in their offspring (17). In humans, *Peg3* biallelic silencing has been observed in endometrial and cervical cancer cell lines and in a number of ovarian cancer and glioma cell lines (10, 18).

Cyclophilin A (CypA),[2] a member of the immunophilin family of proteins, mediates inhibition of calcineurin by the immunosuppressive drug cyclosporine A (CsA), but the other cellular functions of CypA have remained elusive. Recently, different aspects of biological functions of CypA have emerged, suggesting that CypA is involved in multiple signaling events of eukaryotic cells. It might either act as a catalyst for prolyl bond isomerization or form stoichiometric complexes with target proteins. CypA possesses enzymatic peptidylprolyl isomerase activity, which is essential to protein folding *in vivo*. It promotes proper subcellular localization of Zpr1p, regulates interleukin-2 tyrosine kinase activity, and is required for retinoic acid-induced neuronal differentiation in P19 embryonal carcinoma (EC) cells (19–21).

It has been demonstrated that CypA specifically interacts with SIN3-Rpd3 histone deacetylase (HDAC) *in vitro*, suggest-

* This work was supported by Grant CA66746 from the National Cancer Institute. The costs of publication of this article were defrayed in part by the payment of page charges. This article must therefore be hereby marked "*advertisement*" in accordance with 18 U.S.C. Section 1734 solely to indicate this fact.

[1] To whom correspondence should be addressed. Tel.: 310-825-0535; E-mail: rchiu@dent.ucla.edu.

[2] The abbreviations used are: CypA, cyclophilin A; ChIP, chromatin immunoprecipitation; CsA, cyclosporine A; EC, embryonal carcinoma; HDAC, histone deacetylase; QRT, quantitative real-time; WT, wild type; KD, knockdown; KO, knockout; RNAi, RNA interference; Dnmt, DNA methyltransferase.

ing that CypA affects gene expression by physically interacting with HDAC (22). In screening for the gene(s) responsible for the alteration of phenotype in *CypA*-KD P19 cells (21), we observed a silent paternally expressed gene, *Peg3*. Subsequently, we found an inverse relationship between mRNA expression and DNA hypermethylation as well as *Peg3* reactivation from *CypA*-KD P19 cells by demethylation reagents and HDAC inhibitor, suggesting that epigenetic mechanisms play an important role in the regulating of *Peg3* expression in *CypA*-KD P19 cells. Chromatin immunoprecipitation (ChIP) assays indicated a loss of acetylation and a gain of lysine 9 trimethylation in histone 3, as well as enhanced DNA methyltransferase 1 (Dnmt1) and MBD2 binding on the CpG islands of *Peg3* in *CypA*-KD P19 cells. Our data demonstrate the epigenetic function of CypA, which protects the paternal allele of *Peg3* from DNA methylation and inactive histone modifications.

MATERIALS AND METHODS

RNA Isolation, cDNA Synthesis, and Quantitative Real-time (QRT)-PCR—Total RNA samples were isolated from 3×10^6 cells by using the RNeasy Mini Kit (Qiagen) with on-column DNase digestion according to the manufacturer's protocols. Oligo(dT)-primed cDNA was synthesized from 3 μg of RNA using SuperScript™ (Invitrogen). The 20-μl products of reverse transcription were diluted to 40 μl, and 2 μl were used for each PCR reaction. PCR reactions were performed in a total volume of 25 μl containing 2 μM primers and 12.5 μl of the Power SYBR green PCR master mix (Applied Biosystems). The primers used in real-time PCR were c*Peg3*-F (5′-GCCTAAACCAACCCAT-AATGTC-3′) and c*Peg3*-R (5′-CTGAAAGAGT-CCCTGCGTTC-3′). As an input control, glyceraldehydes-3-phosphate dehydrogenase (GAPDH) was amplified using the following primers: GAPDH-F (5′-CAGTGGCAAAGTGG-AGATTG-3′) and GAPDH-R (5′-AATTTGCCG-TGAGTGGAGTC-3′)S. QRT-PCR was performed under the following conditions: 95 °C for 10 min for the initial denaturing followed by 40 cycles of denaturing at 95 °C for 20 s, annealing at 60 °C for 30 s, and extension at 72 °C for 30 s. The data were analyzed using the function $2^{-\Delta\Delta CT}$, where $\Delta\Delta CT = (CT, Target - CT, GAPDH)_{sample} - (CT, Target - CT, GAPDH)_{calibrator}$. In our experiments, GAPDH was used as an internal control to normalize PCR for the amount of RNA added to the reverse transcription reactions. We arbitrarily used wild type (WT P19) cells as a calibrator while using KD (*CypA* knockdown P19) cells as a sample to indicate the relative difference. Primer and template designs followed the same criteria for each target, and primers and Mg^{2+} concentrations had been optimized to render efficiency for each target near one per assumption underlying the $2^{-\Delta\Delta CT}$ method.

Genomic Bisulfite Sequencing and Methylation-specific PCR—Genomic DNA was isolated using the DNeasy Tissue Kit (Qiagen) according to the manufacturer's instructions. Two μg of DNA were digested with EcoRI, extracted with phenol-chloroform, and then subjected to sodium bisulfite conversion, using the EZ DNA methylation Kit (ZYMO Research). The converted DNA was diluted to 20 μl, and 4 μl were used for each PCR reaction. To amplify all of the CpG islands for bisulfite sequencing, regardless of methylation status, unbiased primers *Peg3* S-F (forward, 5′-GTAGTTTGATTGGTAGGGTG-3′) and *Peg3* S-R (reverse, 5′-CAATCTACAACCTTATCAATT-AC-3′) were used to perform PCR under the following conditions: 95 °C for 10 min for the initial denaturing followed by 40 cycles of denaturing at 95 °C for 20 s, annealing at 60 °C for 30 s, and extension at 72 °C for 30 s. To monitor the efficiency of bisulfite treatment, the PCR products were subcloned into the TA cloning vector, and 15 different clones were sequenced individually. If >95% of cytosine was converted into thymidine, we selected those DNA samples for bisulfite sequencing analyses. Methylation-specific PCR was performed using primers *Peg3* M-F (5′-AGACGTTGGGGAGTTAGGAG-TCGC-3′) and *Peg3* M-R (5′-TATAATCTACCG-CCCCTAACCCGCG-3′) for methylated DNA and primers *Peg3* U-F (5′-AGATGTTGGGG-AGTTAGGAGTTGT-3′) and *Peg3* U-R (5′-TATAATCTACCACCCCTAACCCACA-3′) for unmethylated DNA. PCR conditions were 95 °C for 3 min for the initial denaturing followed by 35 cycles of denaturing at 95 °C for 30 s, annealing at 60 °C for 1 min, and extension at 72 °C for 1 min. To directly observe bands representing methylated and unmethylated DNA, PCR products were resolved on a 2% agarose gel and visualized by ethidium bromide staining.

ChIP Analysis—ChIP assays were carried out using a kit from Upstate according to the manufacturer's instructions. For Dnmt1 ChIP, cells were treated for 2 h with 5 μM 5-aza-dC to arrest the fleeting covalent association of methyltransferase with the DNA substrate. Briefly, 1×10^7 cells were used per ChIP assay. After 10 min of 1% formaldehyde treatment, the cells were harvested and sonicated for 3×20 s using a Tekmar sonic disrupter set to 30% of maximum power to produce soluble chromatin, with average sizes between 300 and 1000 bp. The chromatin samples were then diluted 8-fold in the dilution buffer and precleaned for 1 h using 75 μl of salmon sperm DNA/protein A- or G-agarose beads. Ten μg of antibodies were then added to each sample and incubated overnight at 4 °C. To collect the immunocomplex, 60 μl of salmon sperm DNA/protein A- or G-agarose beads were added to the samples for 1 h at 4 °C. The beads were washed once in each of the following buffers, in order: low salt, high salt, and LiCl immune complex wash buffer; they were then washed twice in TE buffer (10 mM Tris-HCl, 1 mM EDTA, pH 8.0). The bound protein-DNA immunocomplexes were eluted twice with 250 μl of elution buffer and subjected to reverse cross-linking at 65 °C for 6 h. The reverse cross-linked chromatin DNA was further purified by proteinase K digestion and phenol-chloroform extraction. DNA was then precipitated in ethanol and dissolved in 20 μl of TE buffer. Two microliters of DNA were used for each QRT-PCR with primers g*Peg3*-F (5′-ACCCTGAC-AAGGAGGTGTCCC-3′) and g*Peg3*-R (5′-GTCTAGTGCACCCACACTGAAC-3′). For a positive control, RNA polymerase II antibody was used to immunoprecipitate actively expressed promoter, and mouse GAPDH promoter was amplified by using primers mGAPDHpF (5′-TACTCGCGGCTTTACGGG-3′) and mGAPDHpR (5′-TGGAACAGGGAGGAGCAG-AGAGCA-3′). QRT-PCR was performed under the following conditions: 95 °C for 10 min for the initial denaturing followed by 40 cycles of denaturing at

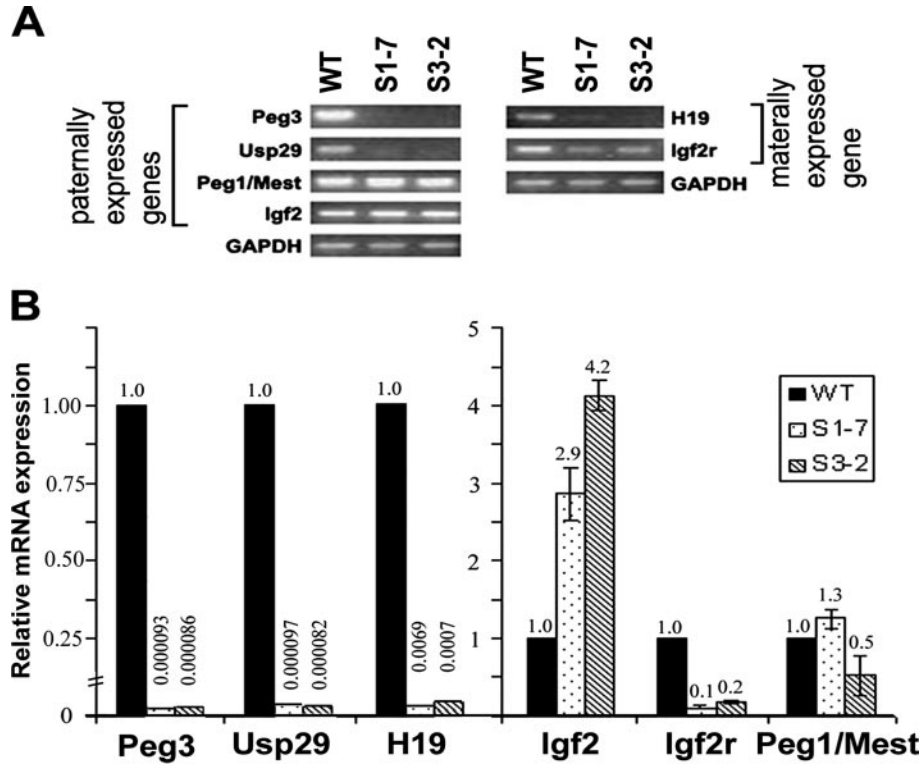

FIGURE 1. ***CypA*-KD selectively affects the expression of imprinted genes.** *A*, semiquantitative reverse transcription-PCR of *Peg3* and other imprinted genes in WT P19 and *CypA*-KD P19 cells. PCR products were subjected to 2% agarose gel electrophoresis. GAPDH was used as an internal control. Shown are WT P19 cells, S1–7, and S3-2 *CypA*-KD stable cell lines. *B*, QRT-PCR analysis of the expression of imprinted genes. GAPDH was used as an internal control to normalize PCR for the amount of RNA added to the reverse transcription reactions. Expression of imprinted genes from WT cells was set as 1, whereas those from KD cells were relative to that of WT, as indicated on the *top* of each bar graph.

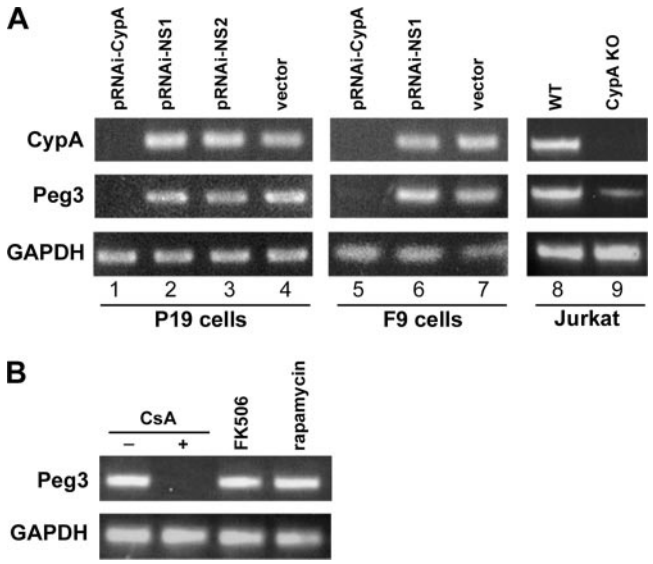

FIGURE 2. ***Peg3* expression is CypA-dependent.** *A*, transiently knocked down *CypA* and knocked out *CypA* resulted in silencing of *Peg3*. pRNAi-*CypA* (S1) (21) was transfected transiently into P19 and F9 cells. Scrambled nonspecific sequences, NS1 and NS2, and empty vector were transfected in parallel as negative controls. Semiquantitative reverse transcription-PCR was performed to measure *CypA* and *Peg3* mRNA expression from transiently transfected P19, F9, and *CypA*-KO Jürkat cells. GAPDH was used as an internal control. *B*, inactivation of peptidylprolyl isomerase activity of CypA resulted in repression of *Peg3* expression. WT P19 EC cells were treated with CsA (1 μg/ml), FK506 (100 ng/ml), or rapamycin (100 ng/ml) or left untreated for 72 h. Semiquantitative reverse transcription-PCR was used to measure *Peg3* expression with GAPDH as an internal control.

95 °C for 20 s, annealing at 60 °C for 30 s, and extension at 72 °C for 30 s. The data were analyzed using the function $2^{-\Delta\Delta CT}$, where $\Delta\Delta CT = (CT, IP - CT, input)_{sample} - (CT, IP - CT, input)_{calibrator}$. In our experiments, input was used as an internal control to normalize PCR for the amount of chromatin DNA added to the ChIP assay. We arbitrarily used WT P19 cells as a calibrator; whereas KD (*CypA*-knockdown P19) cells were compared with WT to generate the relative difference.

RESULTS

Cyclophilin A Knockdown (CypA-KD) Selectively Affects the Expression of Imprinted Genes—To identify genes that could be affected by the *CypA*-KD in P19 EC cells, we found repressed *Peg3* in *CypA*-KD P19 EC cells (S1–7) by using subtraction-differential screening of the subtractive library. Undetectable *Peg3* expression was also exhibited in the other stable *CypA*-KD clone S3-2, suggesting that suppression of *Peg3* resulted from the knocking down of *CypA* (Fig. 1*A*).

To determine whether *CypA*-KD also affects the expression of other imprinted genes, we performed semiquantitative reverse transcription-PCR as well as QRT-PCR to detect *Usp29*, *Peg1/Mest*, *Igf2*, *H19*, and *Igf2r*, using specific primers (Fig. 1). Again, we observed that *Usp29* expression levels were undetectable, suggesting that *Usp29* shares the same imprinting control region with *Peg3* and coordinates silencing of the imprinted transcript *Usp29* with *Peg3*. *H19* localized in a different locus was also undetectable, suggesting that cells lacking the CypA switch expressed *H19* to silence. QRT-PCR analysis clearly demonstrated a 3–4-fold increase in *Igf2*, reduced *Igf2r* mRNA, but no effect upon *Peg1/Mest* expression in S1–7 and S3-2 cell lines (Fig. 1*B*). Collectively, these findings indicate that *CypA*-KD can selectively affect the expression of certain imprinted genes.

Peg3 Expression Is CypA-dependent—Results from the stable *CypA*-KD clones S1–7 and S3-2 clearly demonstrated that knockdown of *CypA* resulted in suppression of *Peg3*. To rule out the possibility that the observed changes resulted from clonal selection, we performed transient transfection of pshRNA-*CypA* into WT P19 EC and F9 EC cells (Fig. 2*A*). Nonspecific short hairpin RNA (shRNA) and an empty vector were used as negative controls. Our results demonstrated that the silencing of *Peg3* is accompanied by transient *CypA*-KD in both P19 EC and F9 EC cells, confirming our hypothesis that *CypA*-KD alone causes *Peg3* silencing and suggesting further that the mechanism may be a general phenomenon in EC cells. To determine whether *CypA*-knockout (KO) also results in

repression of *Peg3* expression, we measured *Peg3* expression from *CypA*-KO Jürkat cells (a generous gift from Dr. Jeremy Luban) using semiquantitative reverse transcription-PCR. As shown in Fig. 2*A*, *lane 9*, we detected low levels of *Peg3* as compared with those in wild type Jürkat cells. Together, these data clearly demonstrate that *Peg3* expression is CypA-dependent.

CypA Isomerase Activity Is Required to Maintain Expression of Peg3—To determine whether CypA isomerase or FK506-binding protein isomerase activity is required to maintain expression of *Peg3*, WT P19 cells were treated with 1 μg/ml CsA and FK506 (100 ng/ml) or rapamycin (100 ng/ml), which inhibits the isomerase activity of CypA and FKBPs, respectively. After 72 h of CsA, FK506, or rapamycin treatment, the cells were harvested to prepare total RNAs. Two μg of total RNA were used to perform RT-PCR to detect *Peg3* using a pair of specific primers. Only CsA-treated WT P19 cells had undetectable *Peg3* (Fig. 2*B*), indicating that the isomerase enzymatic activity of CypA is necessary for *Peg3* expression.

Silencing of Peg3 Is Reactivated by Treating CypA-KD Cells with the DNA Methyltransferase Inhibitor—To determine whether DNA methylation is involved in silencing of *Peg3* in *CypA*-KD P19 EC cells, we treated the S1–7 and S3-2 cell lines for 5 days with 1.0 μM 5-aza-dC, a DNA methyltransferase inhibitor, followed by amplification of the *Peg3* 129-bp fragment using semiquantitative reverse transcription-PCR and QRT-PCR. Fig. 3 shows that, upon 5-aza-dC treatment, the silent *Peg3* gene in S1–7 and S3-2 was reactivated. These results demonstrate an inverse relationship between DNA methylation and *Peg3* expression and support the hypothesis that *Peg3* transcription is regulated by promoter methylation.

CypA-KD Resulted in Biallelic Methylation of CpG Islands Encoded within the Promoter, First Exon, and First Intron of the Peg3 Gene—To directly show methylation of the *Peg3* gene, we used bisulfite modification and DNA sequencing to analyze the methylation status of 445-bp CpG islands encoded within the promoter, first exon, and first intron of this gene (Fig. 4). Analysis of 15 individual clones revealed that, in *CypA*-KD P19 cells, 26 CpG dinucleotides were 98% methylated, indicating biallelic methylation, whereas in WT P19 cells, the methylated CpG islands were at 42.3% frequency, which is consistent with monoallelic methylation of the imprinted gene (Fig. 5*A*). We next performed methylation-specific PCR on sodium bisulfite-modified genomic DNA. Two pairs of primers (U and M) were used for annealing to unmethylated and methylated DNA, respectively. Primers were designed within the *Peg3* CpG islands containing frequent cytosine to distinguish methylated from unmethylated DNA. A biallelic methylation pattern was observed in S1–7 and S3-2, whereas a monoallelic methylation represented by both unmethylated and methylated DNA bands was observed in WT P19 cells (Fig. 5*B*), correlating with the monoallelic methylation of the imprinted gene.

Dnmt1 Is Responsible for Methylation of the Unmethylated Allele of Peg3 in the CypA-KD Cells—To determine whether Dnmt1 is responsible for the methylation of selected DNA targets, an *in vivo* complex of methylation analysis was used as described previously to detect and quantify the physical interaction of Dnmt1 with substrate genomic DNA in a physiological setting in chromatin (23). QRT-PCR analysis of ChIP products generated by immunoprecipitation with antibody against Dnmt1 (Abcam) in the WT P19 and *CypA*-KD P19 cell lines revealed that the Dnmt1-bound DNA fraction in *CypA*-KD P19 cells was ~2.07-fold higher than that of wild type cells (Fig. 6). In contrast, RNA polymerase II-bound GAPDH promoter as a

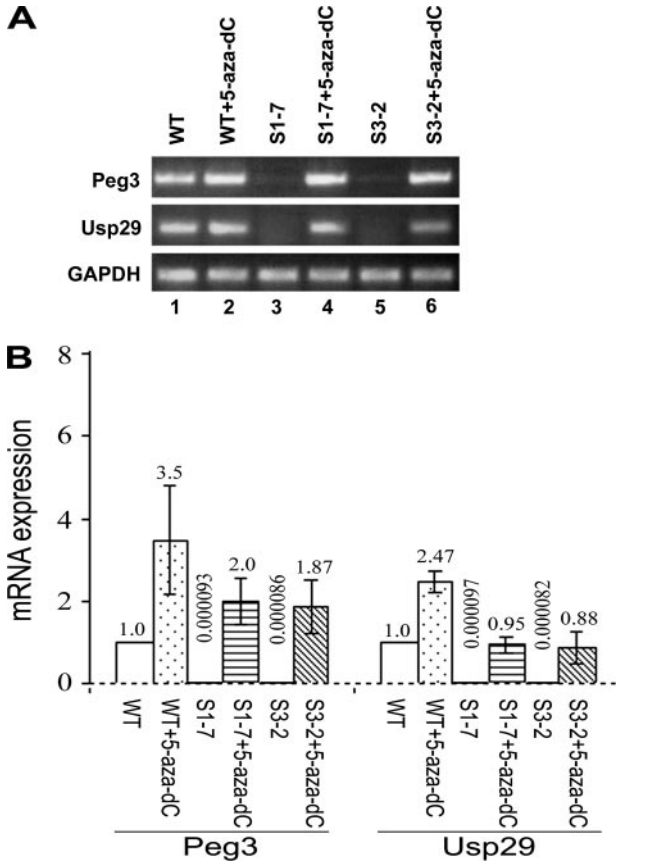

FIGURE 3. **Silent *Peg3* is reactivated by treatment of cells with the DNA methyltransferase inhibitor.** *A*, reactivation of *Peg3* expression is shown by semiquantitative reverse transcription-PCR. Total RNA isolated from 5-aza-dC-treated or -untreated WT-P19, S1–7, and S3-2 cell lines was subjected to reverse transcription-PCR to amplify *Peg3* and *Usp29*. Shown are WT P19 cells and S1–7 and S3-2 *CypA*-KD stable cell lines. *B*, QRT-PCR analysis of expression of *Peg3* and *Usp29* in the presence or absence of 5-aza-dC treatment. Quantitation was achieved by measuring the increase in fluorescence during the exponential phase of PCR. The expression of WT was set as 1, whereas the expression levels of others were relative to the control, as indicated on the *top* of each bar graph.

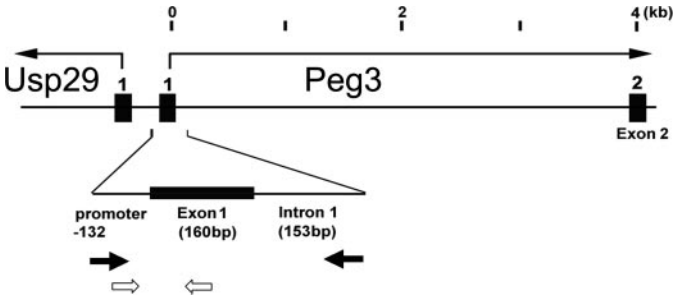

FIGURE 4. **The schematic genomic structure of *Usp29* and *Peg3*.** Exons of these two genes are represented by *black boxes*. The transcription of each gene is indicated by an *arrow*. The positions of the CpG islands encoded within the promoter region, first exon, and first intron are indicated. *Solid* and *open arrows* within the indicated CpG islands are primers for bisulfite sequencing and PCR amplification of ChIP products, respectively.

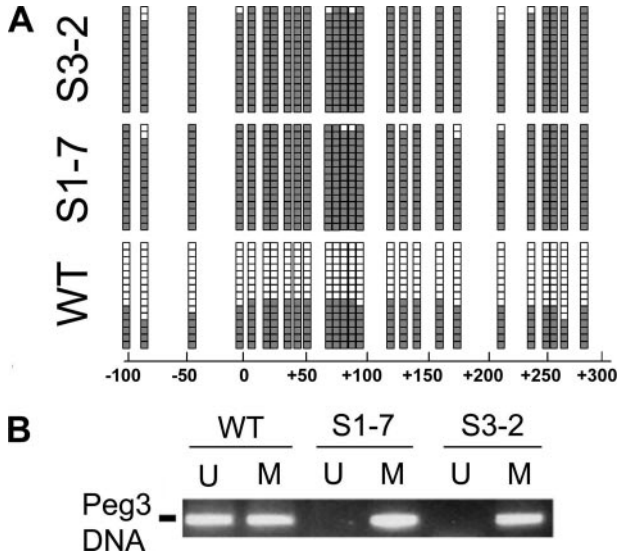

FIGURE 5. **Biallelic methylation of CpG islands within the promoter region, first exon, and first intron of the *Peg3* gene.** *A*, bisulfite sequencing of the *Peg3* CpG islands. The methylation status of each CpG dinucleotide in each clone sequenced is represented as *shaded* and *unshaded boxes* for methylated and unmethylated CpG, respectively. Numbers indicate positions relative to the transcriptional start site. *B*, methylation-specific PCR (MSP) analysis of *Peg3* CpG islands. The sodium bisulfite-treated DNA was subjected to PCR using specific primers for methylated DNA (*M*) and unmethylated DNA (*U*) amplification.

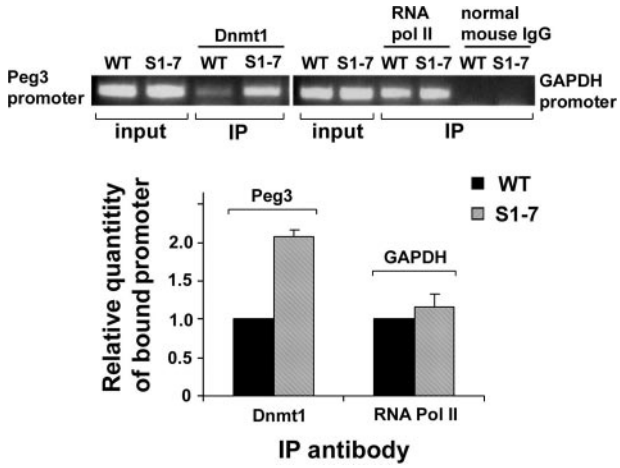

FIGURE 6. **Quantitative analysis of Dnmt1-bound *Peg3* promoter region.** Input and ChIP products were analyzed by semiquantitative PCR. Antibody against RNA polymerase II and normal mouse IgG-immunoprecipitated DNA was amplified with primers of GAPDH promoter to serve as a positive and negative control, respectively. The relative amount of Dnmt1-bound *Peg3* promoter and exonic CpG islands was measured by QRT-PCR.

positive control showed no significant difference between the two cell lines (Fig. 6). These results further substantiate the hypothesis that *CypA*-KD mediates biallelic methylation of the *Peg3* promoter and the first exon.

Partial Relief of the Repressed Peg3 in CypA-KD Cells by Treatment of Cells with the HDAC Inhibitor—It has been well established that the methyl-CpG-binding protein silences transcription by recruiting the HDAC-repressive machinery, which removes acetyl groups from histone, resulting in gene silencing (24, 25). To determine whether histone deacetylation is involved in silencing *Peg3* in *CypA*-KD P19 EC cells, because HDAC binds to CypA (Fig. 7*A*), the S1–7 and S3-2 cell lines

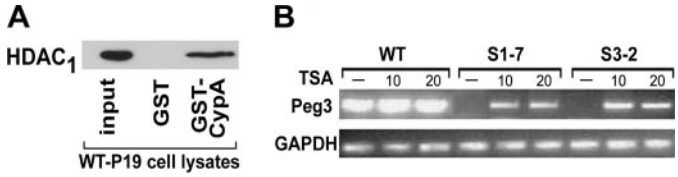

FIGURE 7. **Role of CypA in binding of methylcytosine-binding protein and histone modification of the *Peg3* gene.** *A*, CypA physically interacts with HDAC *in vitro*. Glutathione *S*-transferase (GST)-CypA pulldown of P19 whole cell extracts was performed. The resultant complex was detected with anti-$HDAC_1$ (Santa Cruz Biotechnology) using Western blot analysis. GST-2T was used as a negative control. 1% of the inputs were used as a positive control for HDAC. *B*, partial relief of the repressed *Peg3* in *CypA*-KD cells by treatment of cells with HDAC inhibitor trichostatin A (*TSA*) (10 ng/ml or 20 ng/ml)-treated or -untreated cells are indicated. PCR-amplified GAPDH was used as an internal control.

were treated for 3 days with 10 or 20 ng/ml trichostatin A, a histone deacetylase inhibitor, followed by amplification of the *Peg3* 129-bp fragment using semiquantitative reverse transcription-PCR. Our data demonstrated that trichostatin A only partially relieves *CypA*-KD-mediated *Peg3* repression (Fig. 7*B*). This partial relief indicates that additional mechanisms of repression by methyl-CpG repressory complexes might exist in addition to the recruitment of histone deacetylation. We therefore examined various histone modifications in the *Peg3* promoter of WT P19 and *CypA*-KD P19 cells by ChIP assays, using antibodies against modified histones (acetyl Lys-H3 and trimethyl Lys-9-H3) followed by QRT-PCR analysis.

Reciprocal Pattern of Acetyl Lys-H3 and Trimethyl Lys-9-H3 Was Enriched in the CypA-KD Cells—Histone acetylation was observed in both WT P19 and *CypA*-KD P19 cells but with a 33% weaker signal in *CypA*-KD P19 cells (Fig. 8*A*). Our results suggest that a less-acetylated histone binds to the *Peg3* promoter in the *CypA*-KD P19 cell line S1–7, which correlates with repressed *Peg3* expression in this cell line. The level of trimethyl Lys-9-H3 in the *CypA*-KD cells was ~2.5× greater than that in WT P19 cells, which were set as 50/50 for two parental alleles (Fig. 8*A*), indicating a gain of histone methylation on the *Peg3* promoter. A positive control, GAPDH promoter bound by RNA polymerase II, showed no significant difference between WT- and *CypA*-KD cell lines (Fig. 8*A*). In a pattern reciprocal to that of acetyl Lys-H3, trimethyl Lys-9-H3 was enriched exclusively in the *CypA*-KD P19 cell line. This predominant enrichment of the trimethylation of Lys-9-H3 correlated with the inverse relationship of paternally expressed *Peg3* in WT P19 cells and biallelic methylation and silencing in *CypA*-KD P19 cells. We conclude that silencing of *Peg3* in the *CypA*-KD P19 cell line correlates with a gain of trimethyl Lys-9-H3 on the promoter region of the paternal allele.

MBD2 Is Involved in the Silencing of Peg3 Expression—Our data demonstrate that P19 EC cells have abundant MBD2, which also binds to CypA (Fig. 8*B*). It has been demonstrated that MBD2 is associated with HDACs in the MeCP1 repressor complex (26). To determine whether silencing of the hypermethylated *Peg3* gene is consistent with a model involving methyl-CpG-binding proteins, ChIP analysis was used to study the occupancy of the methylated *Peg3* promoter by MBD2 in the *CypA*-KD P19 cell line as compared with WT P19 EC cells. QRT-PCR analysis of ChIP products generated by immunoprecipitation with an antibody against MBD2 in the WT P19 and

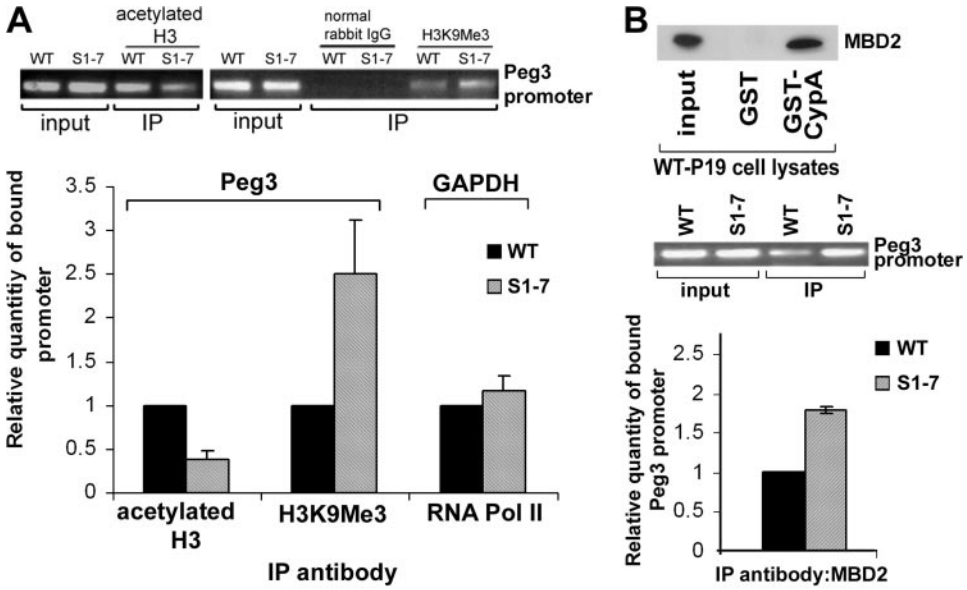

FIGURE 8. **Reciprocal association of acetylated H3 and trimethylated Lys-9-H3 in WT P19 *versus* *CypA*-KD cells.** *A*, relative amounts (immunoprecipitation (*IP*)/input) of acetylated H3 or trimethylated Lys-9-H3 bound to *Peg3* promoter and exonic CpG islands are shown, with *error bar* indicating variation in triplicate experiments. Normal rabbit IgG bound to *Peg3* promoter was used as a negative control. RNA polymerase II antibody-immunoprecipitated DNA was amplified with primers of GAPDH promoter to serve as a positive control. *B*, CypA physically interacts with MBD2 *in vitro*, and quantitative analysis of MBD2-bound *Peg3* promoter and the first exon CpG islands in WT P19 and *CypA*-KD cell line, S1–7. Glutathione *S*-transferase (GST)-CypA pulldown of P19 whole cell extracts was performed. The resultant complex was detected with anti-MBD2 antibody (Upstate) using Western blot analysis 10% of the inputs was used as a positive control. Input and ChIP products were analyzed by semiquantitative PCR, and the relative amounts of MBD2-bound *Peg3* promoter and exonic CpG islands were measured by QRT-PCR.

CypA-KD P19 cell lines revealed the MBD2-bound DNA fraction in the *CypA*-KD P19 cell lines was ~1.8-fold higher than that in WT-P19 cells (Fig. 8*B*), suggesting that MBD2 is involved in the silencing of *Peg 3* expression.

DISCUSSION

Using a revolutionary RNA interference (RNAi) technique, we have been able to analyze loss-of-function phenotypes for the first time to define the function of CypA, which is required to maintain the differential methylation of the CpG islands and histone modification in the promoter and its extended exonic region of the *Peg3* gene. Although off-target effects have been documented during RNAi experiments and integration of an RNAi vector, this is not the case in our presented data. Based on the BLAST sequence data base, we did not find any other sequence identical to our designed targeting site, as described previously (21). In addition, using a nonspecific sequence of shRNA (Fig. 2*A*, *NS1* and *NS2*) and an empty vector as a negative controls did not result in the silencing of *Peg3*, suggesting that our observation was of *CypA*-KD-mediated effects.

Double-stranded RNA derived from a processing of RNAi can also produce transcriptional gene silencing in *Arabidopsis*, *Schizosaccharomyces pombe*, and mammalian cells (27–29). Transcriptional gene silencing mediated by double-stranded RNAs was shown to be due to RNA-dependent DNA methylation. RNA-dependent DNA methylation requires a double-stranded RNA to target DNA and is subsequently processed to yield short RNAs. These short double-stranded RNAs happened to include sequences identical to genomic promoter regions and in turn proved capable of inducing methylation of the homologous promoter and subsequent transcriptional gene silencing. Once again, we conducted a sequence BLAST search, and there were no sequences identified in the promoter region and first exon of the *Peg3* gene identical to S1, which was used to target *CypA* (21).

In this report, results from the stable *CypA*-KD clones S1–7 and S3-2 clearly demonstrated that suppression of *Peg3* resulted in cells lacking CypA. Silencing of *Peg3* was also accompanied by transient knockdown *CypA* in both P19 and F9 embryonal carcinoma cells, indicating that the observed silent *Peg3* does not result from clonal selection. Furthermore, treatment of P19 cells with CsA, an isomerase inhibitor, resulted in silencing of *Peg3*, suggesting that the isomerase enzymatic activity of CypA is necessary for *Peg3* expression.

In contrast, treatment of P19 cells with FK506, rapamycin, FKBP isomerase blocking agents, did not affect *Peg3* expression. These results further substantiate the notion that the isomerase enzymatic activity of CypA (and not FKBPs or calcineurin phosphatase activity) is required for *Peg3* expression. In addition, data obtained from *CypA*-KO Jürkat cells clearly demonstrated that *Peg3* expression is CypA-dependent (Fig. 2*A*). An attempt to rescue the silent *Peg3* with a *CypA* cDNA expression plasmid that is not targetable by the RNAi-*CypA* failed (data not shown). This failure to rescue implicated that the irreversible covalent bond modification of DNA methylation has been established.

The inverse relationship between mRNA expression and DNA hypermethylation as well as our findings of *Peg3* reactivation by demethylation agents suggest that this epigenetic mechanism plays an important role in *Peg3* regulation in *CypA*-KD P19 cells. Epigenetic switches consist of both DNA methylation and histone methylation (6). Bisulfite genomic sequencing and MSP analysis clearly demonstrated a biallelic methylation of CpG islands within the promoter region, first exon, and first intron of the *Peg3* gene in *CypA*-KD P19 cells, whereas methylation of this region in the WT P19 cells remains monoallelic (Fig. 5). CpG methylation at any critical site may increase the likelihood of binding of methylcytosine-binding proteins, which can recruit HDACs and H3-Lys-9 methyltransferase to mediate inactive chromatin remodeling. We hypothesized that MBD2 associates with methylated DNA within the promoter region of the repressed *Peg3* gene. ChIP analysis with MBD2 antibody showed that more MBD2 was associated with the promoter region of *Peg3* in the *CypA*-KD P19 cells (Fig. 8*B*). Additionally, a reciprocal pattern of acetyl Lys-H3 and trimethyl

Lys-9-H3 was enriched in the *CypA*-KD cells compared with WT P19 cells, as indicated by ChIP assays (Fig. 8*A*). Trimethylation of histone 3 on Lys-9 provides a histone code indicative of inactive chromatin structure. Therefore, DNA methylation is both a cause for and a result of heterochromatinization. Methylation patterns depend upon the activity of DNA methyltransferases. A Dnmt activity assay using a synthetic template, poly(dI-dC)-poly(dI-dC), showed no increase in global Dnmt activities (data not shown), whereas the Dnmt1-bound *Peg3* promoter is 2.07-fold higher in the *CypA*-KD cells than than in WT P19 cells (Fig. 6). Collectively, our data indicate that selective hypermethylation of DNA might have occurred in the *CypA*-KD cells, and Dnmt1 is involved in at least the maintenance of this hypermethylation. CypA may be necessary to retain a modulator, which is required for maintenance of imprinting gene expression, in the inactive cytoplasmic form as reported previously for the function of Hsp90 in chromatin remodeling (30, 31). The precise temporal and spatial control of imprinting gene expression may be altered when cells lack CypA.

It has been reported that DNA methylation patterns are remarkably stable and change little with the *in vitro* culture of cancer cell lines (32). In this study, we have demonstrated a simple epigenetic switch for *Peg3* by knocking down *CypA*. The precise mechanism underlying this switch remains to be elucidated. It is possible that the lack of isomerase activity of CypA leads to a global redistribution of factors required for epigenetic modifications. Inactivation of *Peg3* by hypermethylation likely confers a survival advantage, as *Peg3* regulates the translocation of the proapoptotic Bax from cytoplasm to the mitochondria (33). *CypA*-KD P19 cells are indeed less sensitive to retinoic acid plus BMP4-induced apoptosis as compared with wild type cells.[3] *Peg3* hypermethylation has been reported in gliomas, and re-expression of a *Peg3* cDNA in glioma cell lines resulted in a loss of tumorigenecity in nude mice, suggesting that this gene production functions as a tumor suppressor (34). Taken together, this epigenetic alteration would seem to provide *CypA*-KD P19 cells with cell survival advantages compared with wild type cells. This statement is also supported by our previous data indicating that *CypA*-KD cells have a faster growth rate than wild type P19 cells (21).

Acknowledgments—We thank the UCLA Sequencing and Genotyping Core Facility for DNA sequencing and real-time PCR, Jeremy Luban for CypA-KO Jürkat cells, and members of the R. Chiu and G. Fan laboratories for technical assistance and comments.

REFERENCES

1. Bird, A. (2002) *Genes Dev.* **16,** 6–21
2. Li, E. (2002) *Nat. Rev. Genet.* **3,** 662–673
3. Reik, W., and Walter, J. (2001) *Nat. Rev. Genet.* **2,** 21–32
4. Surani, M. A. (1998) *Cell* **93,** 309–312
5. Razin, A., and Kantor, B. (2005) *Prog. Mol. Subcell. Biol.* **38,** 151–167
6. Li, T., Vu, T. H., Ulaner, G. A., Littman, E., Ling, J. Q., Chen, H. L., Hu, J. F., Behr, B., Giudice, L., and Hoffman, A. R. (2005) *Mol. Hum. Reprod.* **11,** 631–640
7. Amir, R. E., Van den Veyver, I. B., Wan, M., Tran, C. Q., Francke, U., and Zoghbi, H. Y. (1999) *Nat. Genet.* **23,** 185–188
8. Okano, M., Bell, D. W., Haber, D. A., and Li, E. (1999) *Cell* **99,** 247–257
9. Gibbons, R. J., McDowell, T. L., Raman, S., O'Rourke, D. M., Garrick, D., Ayyub, H., and Higgs, D. R. (2000) *Nat. Genet.* **24,** 368–371
10. Maegawa, S., Yoshioka, H., Itaba, N., Kubota, N., Nishihara, S., Shirayoshi, Y., Nanba, E., and Oshimura, M. (2001) *Mol. Carcinog.* **31,** 1–9
11. Jones, P. A., and Baylin, S. B. (2002) *Nat. Rev. Genet.* **3,** 415–428
12. Feinberg, A. P., and Tycko, B. (2004) *Nat. Rev. Cancer* **4,** 143–153
13. Egger, G., Liang, G., Aparicio, A., and Jones, P. A. (2004) *Nature* **429,** 457–463
14. Kim, J., Ashworth, L., Branscomb, E., and Stubbs, L. (1997) *PCR Methods Applications* **7,** 532–540
15. Kuroiwa, Y., Kanekoishino, T., Kagitani, F., Kohda, T., Li, L. L., Tada, M., Suzuki, R., Yokoyama, M., Shiroishi, T., Wakana, S., Barton, S. C., Ishino, F., and Surani, M. A. (1996) *Nat. Genet.* **12,** 186–190
16. Hiby, S. E., Lough, M., Keverne, E. B., Surani, M. A., Loke, Y. W., and King, A. (2001) *Hum. Mol. Genet.* **10,** 1093–1100
17. Li, L. L., Keverne, E. B., Aparicio, S. A., Ishino, F., Barton, S. C., and Surani, M. A. (1999) *Science* **284,** 330–333
18. Dowdy, S. C., Gostout, B. S., Shridhar, V., Wu, X., Smith, D. I., Podratz, K. C., and Jiang, S. W. (2005) *Gynecol. Oncol.* **99,** 126–134
19. Ansari, H., Greco, G., and Luban, J. (2002) *Mol. Cell. Biol.* **22,** 6993–7003
20. Brazin, K. N., Mallis, R. J., Fulton, D. B., and Andreotti, A. H. (2002) *Proc. Natl. Acad. Sci. U. S. A.* **99,** 1899–1904
21. Song, J., Lu, Y. C., Yokoyama, K., Rossi, J., and Chiu, R. (2004) *J. Biol. Chem.* **279,** 24414–24419
22. Arevalo-Rodriguez, M., Cardenas, M. E., Wu, X., Hanes, S. D., and Heitman, J. (2000) *EMBO J.* **19,** 3739–3749
23. Liu, K., Wang, Y. F., Cantemir, C., and Muller, M. T. (2003) *Mol. Cell. Biol.* **23,** 2709–2719
24. Nan, X., Ng, H. H., Johnson, C. A., Laherty, C. D., Turner, B. M., Eisenman, R. N., and Bird, A. (1998) *Nature* **393,** 386–389
25. Jones, P. L., Veenstra, G. J., Wade, P. A., Vermaak, D., Kass, S. U., Landsberger, N., Strouboulis, J., and Wolffe, A. P. (1998) *Nat. Genet.* **19,** 187–191
26. Ng, H. H., Zhang, Y., Hendrich, B., Johnson, C. A., Turner, B. M., Erdjument-Bromage, H., Tempst, P., Reinberg, D., and Bird, A. (1999) *Nat. Genet.* **23,** 58–61
27. Mette, M. F., Aufsatz, W., van der Winden, J., Matzke, M. A., and Matzke, A. J. (2000) *EMBO J.* **19,** 5194–5201
28. Jones, L., Ratcliff, F., and Baulcombe, D. C. (2001) *Curr. Biol.* **11,** 747–757
29. Morris, K. V., Chan, S. W.-L., Jacobsen, S. E., and Looney, D. J. (2004) *Science* **305,** 1289–1292
30. Ruden, D. M., Xiao, L., Garfinkel, M. D., and Lu, X. (2005) *Hum. Mol. Genet.* **14,** R149–R155
31. Soldars, V., Lu, X., Xiao, L., Wang, X., Garfinkel, M. D., and Ruden, D. M. (2005) *Nat.* Genet. **33,** 70–74
32. Turker, M. S., Swisshelm, K., Smith, A. C., and Martin, G. M. (1989). *J. Biol. Chem.* **264,** 11632–11636
33. Deng, Y. B., and Wu, X. W. (2000) *Proc. Natl. Acad. Sci. U. S. A.* **97,** 12050–12055
34. Kohda, T., Asai, A., Kuroiwa, Y., Kobayashi, S., Aisaka, K., Nagashima, G., Yoshida, M. C., Kondo, Y., Kagiyama, N., Kirino, T., Kaneko-Ishino, T., and Ishino, F. (2001) *Genes Cells* **6,** 237–247

[3] Y.-C. Lu, J. Song, H.-Y. Cho, G. Fan, K. K. Yokoyama, and R. Chiu, unpublished data.